3. Numerical Simulation Reactor Research Project

Fusion plasmas are complex systems which involve a variety of physical processes interacting with each other across wide ranges of spatiotemporal scales. In the National Institute for Fusion Science (NIFS), we are utilizing the full capability of the supercomputer system, the Plasma Simulator, and propelling domestic and international collaborations in order to conduct the Numerical Simulation Reactor Research Project (NSRP). Missions of the NSRP are i) to systematize understandings of physical mechanisms in fusion plasmas for making fusion science a well-established discipline and ii) to construct the Numerical Helical Test Reactor, which is an integrated system of simulation codes to predict behaviors of fusion plasmas over the whole machine range.

The Plasma Simulator "Raijin (雷神)" (Fig. 1) began operations in July 2020. It consists of 540 computers, each of which is equipped with eight "Vector Engine" processors. The 540 computers are connected to each other by a high-speed interconnecting network. The computational performance is 10.5 petaflops. The capacities of the main memory and the external storage system are 202 terabytes and 32.1 petabytes, respectively.

Presented below in Figs.2 and 3 are examples of successful results from collaborative simulation research in 2021-2022 on gyrokinetic simulation of multi-scale (ion-scale and electron-scale) turbulence and on optimization of magnetic field configuration, based on continuous helical coils by the optimization code, OPTHECS, respectively. Also, highlighted in the following pages are achievements of the NSRP research task groups on energetic-particle physics, peripheral plasma transport, multi-hierarchy physics, and a basis of simulation science.

(H. Sugama)

Fig. 1 The Plasma Simulator, "Raijin (雷神)"

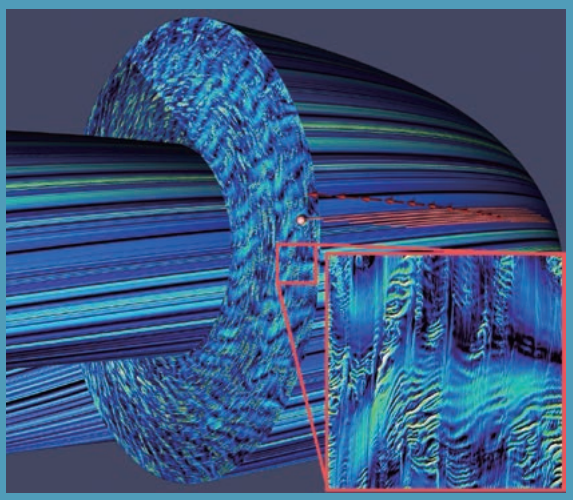

Fig. 2 Perturbed electric field obtained by gyrokinetic simulation of multi-scale (ion-scale and electron-scale) turbulence in a tokamak plasma [presented by Dr. S. Maeyama (Nagoya University)]. Trapped electron motion and magnified perturbation pattern are also shown. Reference: S. Maeyama *et al.*, Nature Communications **13**, 3166 (2022).

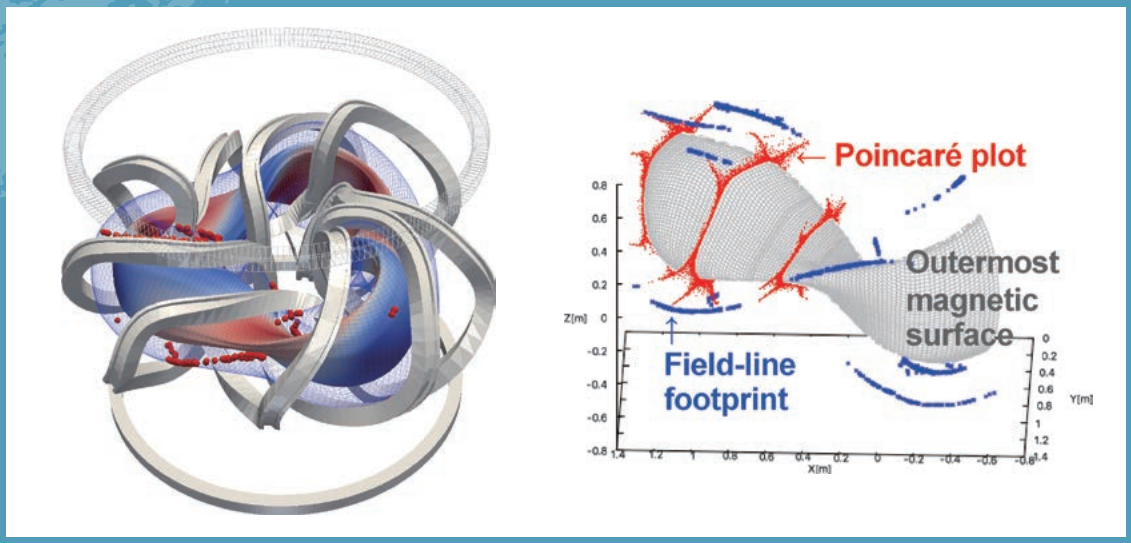

Fig. 3 Optimization of magnetic field configuration based on continuous helical coils by the optimization code, OPTHECS. Low aspect ratio configuration based on quasi-helical symmetry (left) and divertor leg structure created by helical coils (right) [presented by Dr. H. Yamaguchi (NIFS)]. Reference: H. Yamaguchi *et al.*, Nucl. Fusion **61**, 106004 (2021).

Energetic-particle driven instabilities and energetic-particle transport in helical plasmas

Highlight

Simulations of energetic-particle driven instabilities in CFQS

A nonlinear simulation of the energetic-particle (EP) driven instabilities in the Chinese First Quasi-Axisymmetric Stellarator (CFQS) has been conducted for the first time. MEGA, a hybrid simulation code for EPs interacting with a magnetohydrodynamic (MHD) fluid, was used in the present work. Both the m/n = 3/1 energetic particle mode (EPM) and the m/n = 5/2 toroidal Alfvén eigenmode (TAE) were found, where m is the poloidal mode number and n is the toroidal mode number. Four important results were obtained, as follows. First, the instability in the CFQS in three-dimensional form was demonstrated for the first time, as shown in Fig. 1(a). Second, strong toroidal mode coupling was found for the spatial profiles, and it is consistent with the theoretical prediction. Third, the resonant condition caused by the absence of axial symmetry in the CFQS was demonstrated for the first time, as shown in Fig. 1(b) and (c). The general resonant condition is $f_{mode} = Nf_{\varphi} - Lf_{\theta}$, where f_{mode}, f_{φ}, and f_{θ} are mode frequency, particle toroidal transit frequency, and particle poloidal transit frequency, respectively; N and L are arbitrary integers, representing toroidal and poloidal resonance numbers. For the EPM, the dominant and subdominant resonant conditions are $f_{mode} = 3f_{\varphi} - 7f_{\theta}$ and $f_{mode} = f_{\varphi} - f_{\theta}$, respectively. For the TAE, the dominant and subdominant resonant conditions are $f_{mode} = 4f_{\varphi} - 9f_{\theta}$ and $f_{mode} = 2f_{\varphi} - 3f_{\theta}$, respectively. On the one hand, the toroidal resonance numbers (N) are different by two from the toroidal mode numbers (n) for the dominant resonance. This indicates that two-fold rotational symmetry affects the resonance condition. On the other hand, the subdominant resonances satisfy N = n, which is expected for axisymmetric plasmas and most of the toroidal plasmas, including stellarators. Fourth, the nonlinear frequency chirping in the CFQS was demonstrated for the first time. Hole and clump structures were formed in the velocity space of pitch angle and energy, and the particles comprising the hole and clump were kept resonant with the modes during the mode frequency chirping.

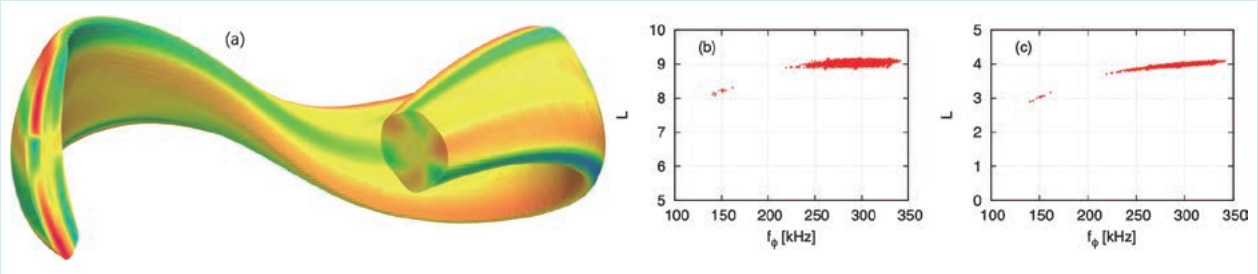

Fig. 1 (a) Radial velocity v_{rad} of the simulated EPM in three-dimensional form. The orange and red represent the velocity from core to edge, while the green and blue represent the velocity from edge to core. (b) The L values of 4096 resonant particles of the TAE for N = 4, where the L = 9 particles represent the dominant resonant condition. (c) The L values of 4096 resonant particles of the TAE for N = 2, where the L = 3 particles represent the subdominant resonant condition.

[1] H. Wang *et al.*, Nucl. Fusion **62**, 106010 (2022).

(H. Wang)

Numerical investigation into the peripheral energetic-particle-driven MHD modes in Heliotron J with free-boundary hybrid simulation

The interaction between EPs and EP-driven MHD instabilities in the Heliotron J, a low-shear helical axis stellarator/heliotron, is investigated with MEGA under a free boundary condition on the last closed flux surface. The m/n = 2/1 EPM and the m/n = 4/2 global Alfvén eigenmode (GAE) in the peripheral plasma region of the Heliotron J are successfully reproduced under the free boundary condition. The free boundary condition affects the EP driving rate of the m/n = 2/1 EPM and the m/n = 4/2 GAE through the changes in the mode spatial profile. Under a fixed boundary condition, the linear growth rate of the EP-driven MHD modes with low mode numbers is underestimated. The interaction between EPs and these experimentally observed modes is kinetically analyzed, as shown in Fig. 2. It is found that the strongest EP-shear Alfvén wave interactions arise from toroidicity-induced resonances in the high-velocity region. These high-velocity EPs have large orbit width, and they can efficiently interact with the peripheral EP-driven mode. Additional toroidally-asymmetric resonances are localized in the low-velocity region; therefore, their effects are weak for the bump-on-tail EP velocity distribution function.

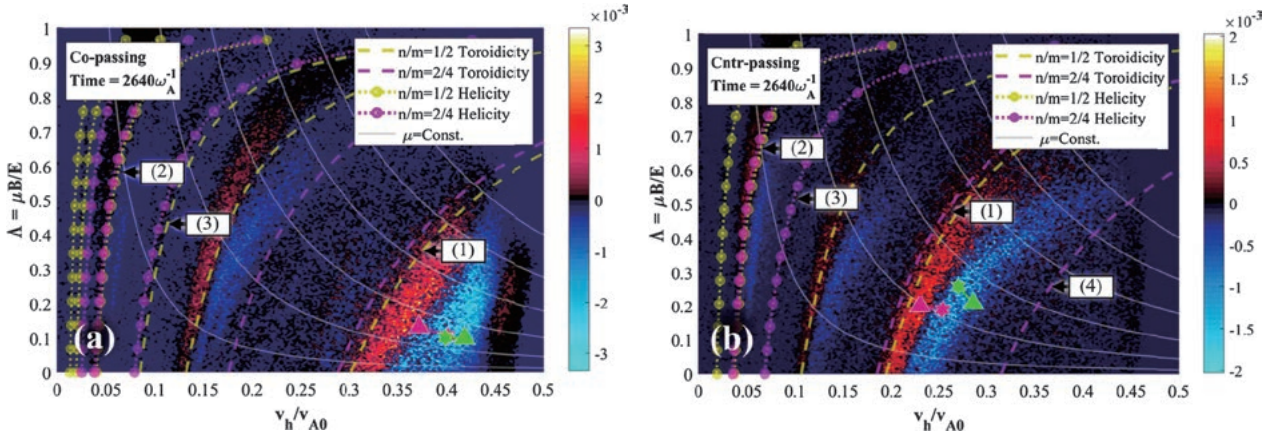

Fig. 2 The EP distribution function variations due to the interaction with EPM and GAE in (v, Λ) phase space, where Λ is the pitch angle. (a) co-passing and (b) counter-passing EPs. The dashed lines and dotted lines with circles represent toroidicity and helicity-induced resonances, respectively. The yellow and purple colors represent the resonant curves for the EPM and GAE, respectively. The purple and green markers indicate the destabilizing and stabilizing resonant EPs with the highest value of |δf|, respectively. The hexagram and triangle indicate the initial and final locations in velocity space of these resonant EPs, respectively.

[2] P. Adulsiriswad *et al.*, Nucl. Fusion **61**, 116065 (2021).

(P. Adulsiriswad)

Simulation study of energetic-particle driven off-axis fishbone instabilities in tokamak plasmas

Hybrid simulations for EPs interacting with MHD fluid were performed to investigate the linear growth and the nonlinear evolution of the off-axis fishbone mode (OFM), destabilized by trapped EPs in tokamak plasmas. The spatial profile of the the OFM is mainly composed of m/n = 2/1 mode inside the q = 2 magnetic flux surface where q is the safety factor, while the m/n = 3/1 mode is predominant outside the q = 2 surface, as shown in Fig. 3(a). The spatial profile of the OFM is a strongly shearing shape on the poloidal plane, suggesting a nonperturbative effect of the interaction with EPs. The frequency of the OFM in the linear growth phase is in good agreement with the precession drift frequency of trapped EPs, and the frequency chirps down in the nonlinear phase. Two types of resonance conditions between trapped EPs and the OFM are found. For the first type of resonance, the precession drift frequency matches the OFM frequency, while for the second type, the sum of the precession drift frequency and the bounce frequency matches the OFM frequency. The resonance frequency, which is defined based on precession drift frequency and bounce frequency of the nonlinear orbit for each resonant particle, is analyzed to understand the frequency chirping. As shown in Fig. 3(b), the resonance frequency of positive δf particles chirps down, which may result in the chirping down of the OFM frequency.

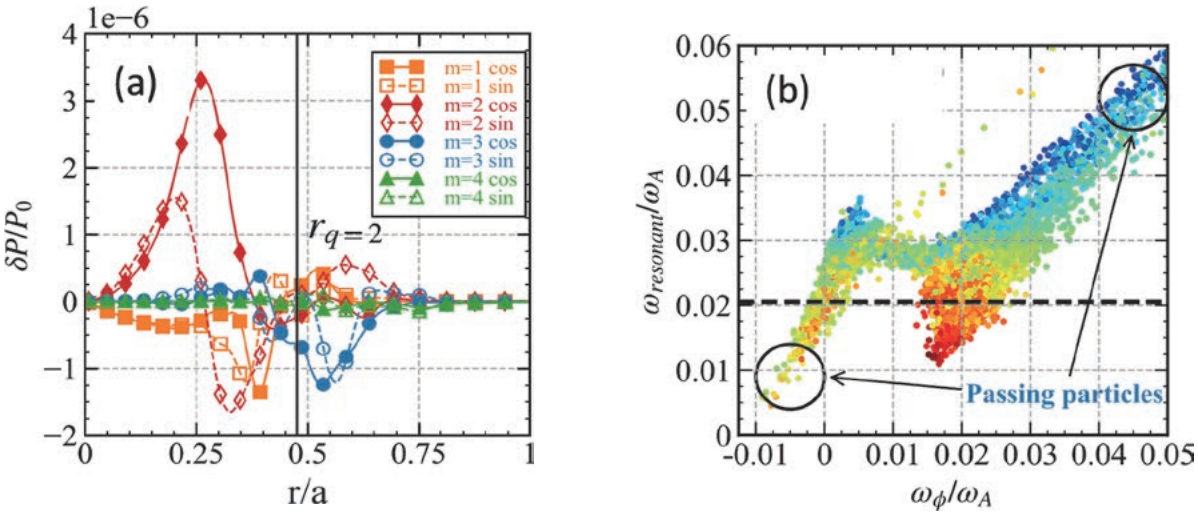

Fig. 3 (a) Radial structures of MHD pressure perturbation at the linear growth phase. The solid (dashed) lines with symbols represent the cosine (sine) parts of Fourier components. The location of the q = 2 magnetic flux surface is denoted by the black solid line. (b) The 8000 particles with the largest |δf| values in (ω_φ, $\omega_{resonant}$) phase space in the nonlinear phase, where ω_φ is particle toroidal orbit frequency and $\omega_{resonant}$ is resonant frequency. Red (blue) color represents positive (negative) δf. The frequency of the OFM is represented by the black dashed line.

[3] H. Li *et al.*, Nucl. Fusion **62**, 026013 (2022).

(H. Li)

New challenges for controlling peripheral plasma transport

Highlight

Divertor configuration control of a quasi-symmetry stellarator by external coils

A new attempt to control the divertor configuration by external coils has been proposed for a stellarator, and its validity has been confirmed by the numerical transport code EMC3-EIRENE. This study has been published [1] and is expected to be one of bases of configuration optimization studies for stellarator devices.

A standard divertor concept has been established for tokamak devices, and many design studies have been performed for many years, while the divertor concept for helical/stellarator devices is not well-established. We installed a set of three external saddle loop coils for each stellarator-symmetry section of a quasi-symmetry stellarator, to control the rotational transform at the edge of the confinement region with closed flux surfaces. The current ratio of the three coils were adjusted to cancel the change of the rotational transform in the core region. We performed a current scan of the external coils, and confirmed the controllability of the confinement region from the connection length distributions shown in Figs. 1(a) and (b); 1) the radial position of the last closed flux surface (LCFS) changes according to the coil current linearly, 2) a positive/negative current increases/decreases the size of the confinement region, and 3) the divertor leg structure outside the LCFS remains and the lengths of the legs change. Steady-state transport calculations were performed for various divertor plate positions, shown in the poloidal cross section in Figs. 1(a) and (b). We use a fixed core electron density and a fixed heating power to see the influence of the divertor configurations on the core electron temperature. The numerical results elucidated the characteristics of divertor configurations; 1) the extension of the leg structure reduces the core temperature because of a smaller core volume and 2) makes the dependence of the divertor plate position on the temperature weaker when the plate is installed outside the LCFS. We concluded that the divertor configuration control for longer divertor legs is effective to reduce the influence of the wall in the core region and to increase the freedom of the divertor plate design.

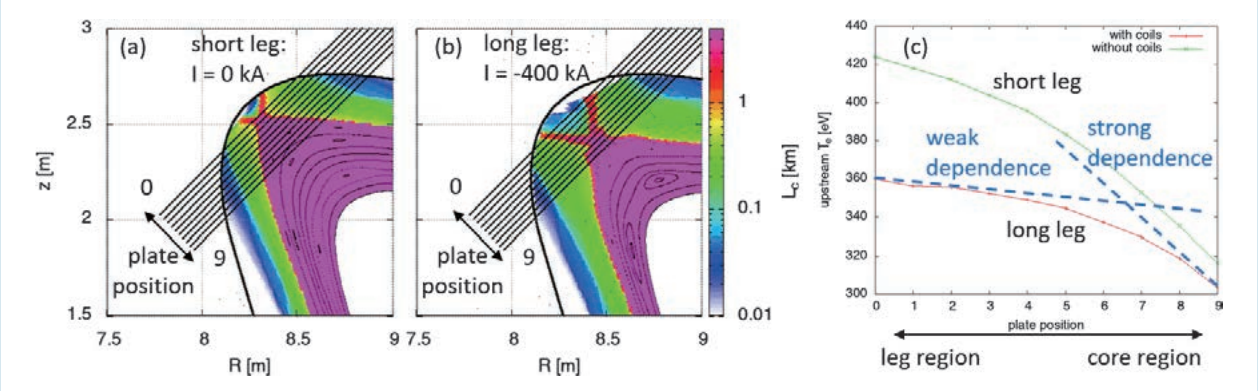

Fig. 1 (a) divertor configuration without coil current and (b) with negative coil current, and (c) dependence of the electron temperature of the core region on the divertor plate position. The two blue dashed lines stand for the gradient of the temperature at the divertor tile positions 0 and 9, in the case of the long leg configuration shown in Fig. 1 (b).

[1] G. Kawamura, M. Nakata, Y. Suzuki, Y. Hayashi, and R. Sakamoto, *"Divertor leg control of a quasi-symmetry stellarator with external coils and its consequences for transport,"* Contrib. Plasma Phys. **62**, e202100196 (2022).

(G. Kawamura)

Particle Simulation of Controlling Particle and Heat Flux by Magnetic Field

An idea for shielding high energy ion and electron fluxes is proposed by applying external magnetic fields [2]. In this work, we model a flowing plasma in a small region by utilizing one spatial dimension and three coordinates for velocities, (the 1D3V) Particle-In-Cell (PIC) code. The plasma which consists of ions and electrons is produced from the source region and absorbed at the conductor wall. The external magnetic field is modified by applying a change of magnetic field in the direction perpendicular to the plasma flow. This magnetic field is localized and switched from strong negative values to strong positive ones at several locations in the simulation region. In figure 2 (a), the magnetic field, B_y, is illustrated. The magnetic fields, B_x, and B_z, are constant and are not changed in this simulation. This magnetic field, B_y, is a small value in comparison with the background magnetic field, B_x, along the simulation domain. We found that this localized reversed magnetic field traps the particles and then reduces the particle and heat fluxes to the wall. Figure 2 (b) shows the comparison of particle and heat fluxes with and without changing the magnetic field. Except for the small region near four "magnetic mirrors", total particle flux is reduced approximately by 76.2% and around 78.9% for the energy flux. Based on the modeling results, external localized-reversed magnetic fields can control the particle and heat fluxes to the wall. These results can be applied for shielding high energy ion and electron fluxes to satellites or spacecraft in space.

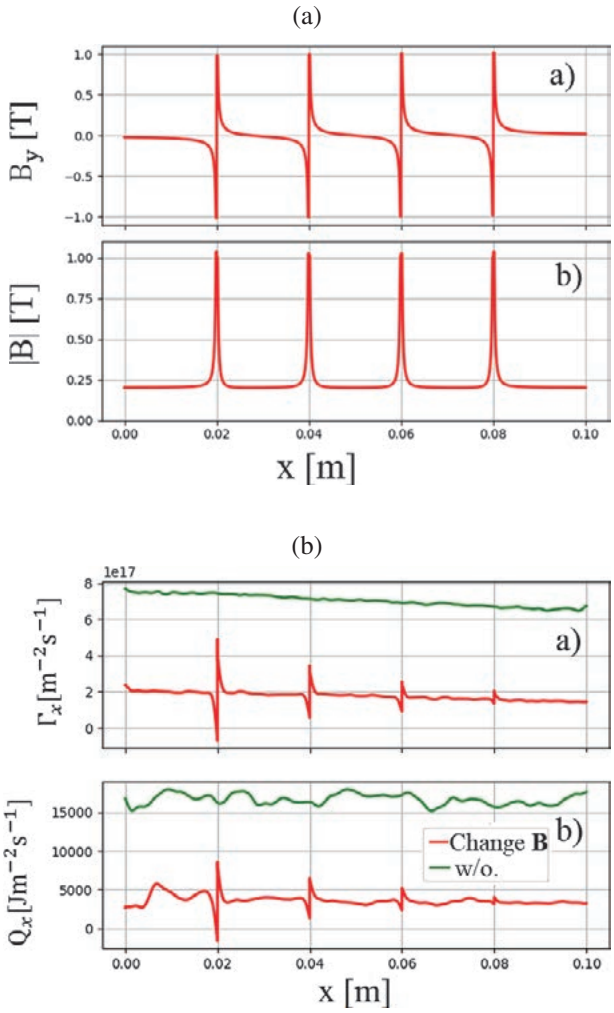

Fig. 2 (a) The analytic function of the magnetic field in y direction and the absolute value of total magnetic field generated by its analytic function in the system. (b) Comparison of one-dimensional total particle flux and energy flux in the case with (red line) and without (green line) changing the magnetic field.

[2] Trang Le, Yasuhiro Suzuki, Hiroki Hasegawa, Toseo Moritaka and Hiroaki Ohtani, *"Particle Simulation of Controlling Particle and Heat Flux by Magnetic Field,"* Plasma Fusion Res. **16**, 1401103 (2021).

(Y. Suzuki, Hiroshima Univ.)

Pseudo-Maxwellian velocity distribution in magnetic reconnection

Highlight

Particle simulations of magnetic reconnection reveal pseudo-Maxwellian velocity distributions, which are almost indistinguishable in shape from a Maxwellian distribution

For realization of fusion on earth, plasma heating to extremely high temperature is required. In a different type of device from LHD, "a spherical tokamak," a heating method via magnetic reconnection is employed. Magnetic reconnection has attracted extensive attention and has been actively studied all round the world. In this study, we investigate magnetic reconnection physics by using our particle simulation code "PASMO." Fig. 1 (a) shows an ion velocity distribution in the downstream region of magnetic reconnection, obtained by the simulation. At first glance, this looks like a Maxwellian velocity distribution, but this is pseudo-Maxwellian, which is almost indistinguishable in shape from a Maxwellian one. Furthermore, we clarify that pseudo-Maxwellian distribution belongs to ring-shaped distribution with a large width [1]. The distribution shape remarkably depends on the width and radius of the ring. When the width is much less than the radius, we can clearly see a ring shape, as displayed in the left case of Fig. 1 (b). As the ring width becomes larger, it is overlapped near the center, and thus the ring's hole is being plugged. If the width is larger than a criterion, the center is transformed from a hole into the peak of a mountain, that is, a pseudo-Maxwellian distribution is formed, as shown in the right case of Fig. 1 (b).

The formation of pseudo-Maxwellian distributions will not be limited to magnetic reconnection. This result means that although a system is not in a thermal equilibrium state, velocity distributions indistinguishable from a Maxwellian one can exist, and has a potential to significantly affect existing knowledge in experiments and observations.

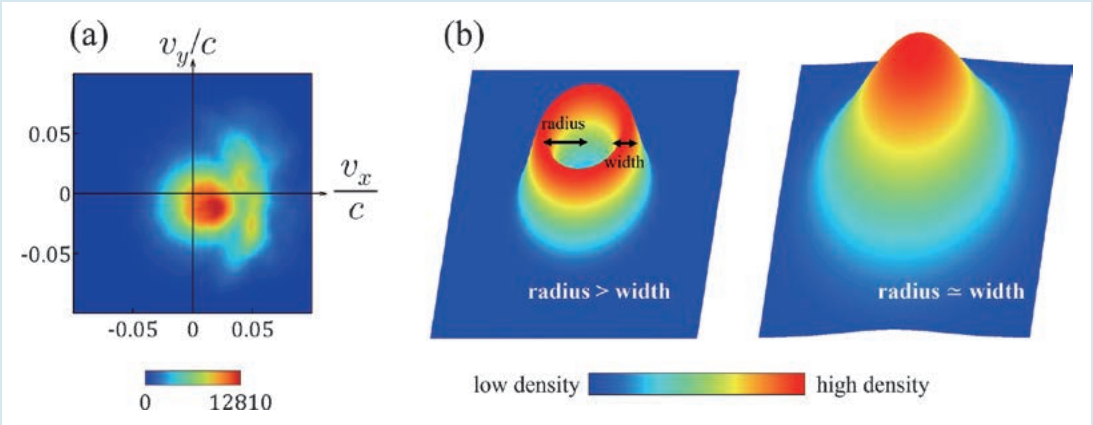

Fig. 1 (a) Pseudo-Maxwellian ion velocity distribution found in a particle simulation, where c is the speed of light. (b)Schematic diagram of velocity distributions (bird's eye view). In the left case, the ring width is much less than the radius, and hence we can clearly see a ring-shaped structure. In the right case, in which the width is nearly equal to the radius, we can see a pseudo-Maxwellian distribution.

[1] S. Usami and R. Horiuchi, Front. Astron. Space Sci. **9**, 846395 (2022).

(S. Usami)

Theoretical Analysis of Cross-field Dynamics on Detached Divertor Plasmas

In order to reduce heat flux into divertor plates, it has been proposed that the plasma is detached from the divertor plates with neutral gases. On the other hand, the correlation between the detachment and cross-field plasma transports has been observed in various magnetic confinement devices. Such a correlation is expected to reduce the maximum heat flux density with an expansion of its width. In this study, we proposed a theoretical model of feedback instability for the mechanism of the correlations. We considered the detached divertor plasma model with both electric currents in the upstream plasma and the detached region. As a result, we found that a feedback instability mode could be induced under a certain condition and that the waves of the unstable mode could transport the plasma across the magnetic field line. We also analyzed the dependences of the feedback instability mode on the total collision frequency and the recombination coefficient in the detached region, as shown in Fig. 2, and that on the density gradient [2,3].

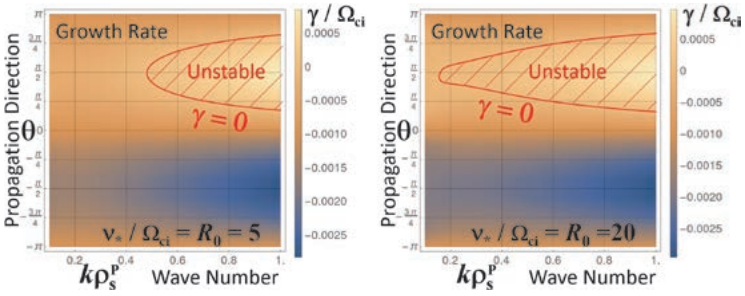

Fig. 2 Dependences of the growth rate of the feedback instability mode on the wave number and the propagation direction with the parameters of a typical fusion torus device. Here the total collision frequency and the recombination coefficient in the detached region for the left panel are lower than those for the right panel.

[2] H. Hasegawa, H. Tanaka, and S. Ishiguro, 28th IAEA Fusion Energy Conference, TH/P4-18 (2021).
[3] H. Hasegawa, H. Tanaka, and S. Ishiguro, Nuclear Fusion **61**, 126005 (2021). (H. Hasegawa)

Isotope effect in multi-ion-species helical plasmas under radial electric fields

Confinement of mixed hydrogen isotope plasmas is necessary for effective fusion reactions in future thermonuclear reactors. We focus on the mass number dependency of ion thermal conductivity, due to the ion temperature gradient mode (Fig. 3) in such multi-ion-species plasmas. The global gyrokinetic code, XGC-S, is employed for quasi-linear estimation of ion thermal conductivity under a global radial electric field in a helical configuration.

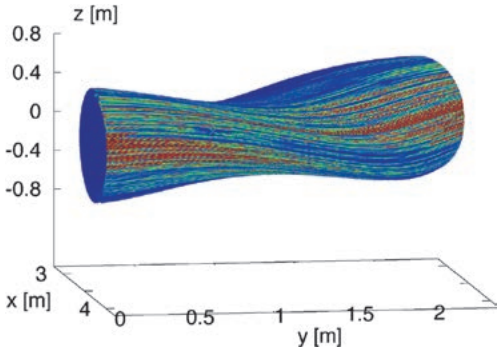

Fig. 3 Potential fluctuations due to ion temperature gradient mode in a helical configuration.

It is found that the heavy hydrogen component effectively enhances the light hydrogen heat flux, which mainly affects the ion thermal conductivity. This effect is evident for light-hydrogen-dominated plasmas with small average mass numbers. As a result, the average mass number dependency becomes more favorable than conventional gyro-Bohm scaling. The radial electric field can affect ion thermal conductivity through mode stabilization and wavelength elongation. In single-ion-species plasmas, these two effects result in the transition from unfavorable gyro-Bohm scaling to favorable mass number dependency. The present simulation study shows that the radial electric field suppresses the ion heat flux, while keeping the favorable mass number dependency in multi-ion-species plasmas. In conclusion, the radial electric field and the heavy hydrogen component potentially realize the favorable mass number dependency, observed in the Large Helical Device and other experimental devices. This result was presented at the 28th IAEA Fusion Energy Conference [4].

[4] T. Moritaka, M. Cole, R. Hager *et al.*, "Isotope effects in ion temperature gradient modes with radial electric field in Large Helical Device", 28th IAEA Fusion Energy Conference, online, May 10–15 (2021). (T. Moritaka)

Visualization analysis of data, and development of simulation methods

Highlight

Visualization of plasma shape in the LHD-type helical fusion reactor, FFHR, by a deep learning technique

A magnetic confinement fusion reactor generates a helical magnetic field to limit plasma in a certain region. To achieve a continuous nuclear reaction, it is important to prevent plasma from having a collision with inner components of the reactor. Therefore, the shape of this region, the plasma shape, is relative to the inner components design of a fusion reactor. To represent the shape of this region, thousands of magnetic field lines are traced in the helical magnetic field and it causes some problems. First, rendering all the lines takes a lot of time. Besides, to check for interferences, it is unnecessary to consider those magnetic field lines buried under other lines. Second, separated lines cannot provide a continuous and clear boundary. Finally, the Larmor radius is hard to represent with lines. Therefore it is suitable to represent plasma shape by a surface. However, due to the helical magnetic field, it lines are twisted and entwined with each other. Regardless of whether the connectivity information of a line has been provided, the relative position information between two lines is extremely complex. Therefore it is difficult to know which lines are contributing to surface generation.

To tackle the challenge, we propose using a deep neural network (DNN) to learn the representation of the plasma shape and to reconstruct a regular scalar field from the magnetic field lines [1]. The intersection points on each poloidal plasma cross-section are used to make annotations, according to the connection length of the magnetic field line to which they belong. Afterward, these labeled points are inputted into a DNN as training material. Therefore the trained DNN can label each point from its new position in the scalar field. Then the scalar field can represent the different parts of the plasma shape by collecting the points with the same label. Since the scalar field has been structured, the magnetic flux intensity at any position of this scalar field is easily obtained. The Larmor radius then can be calculated. The representation of a Larmor radius is embedded in the scalar field. With a scalar field, the marching cubes (MC) method can be used to generate an isosurface for different parts of the plasma shape. The right of Fig. 1 shows a visualization result of a quarter of the plasma shape model. The model accurately reproduces the complicated plasma shape structure. Compared with rendering using line objects, it clearly distinguishes the two areas. Furthermore, because of the surface representation, it enables us to check the interferences directly between the plasma shape model and 3D design data of components in the FFHR, as shown on the right of Fig. 1.

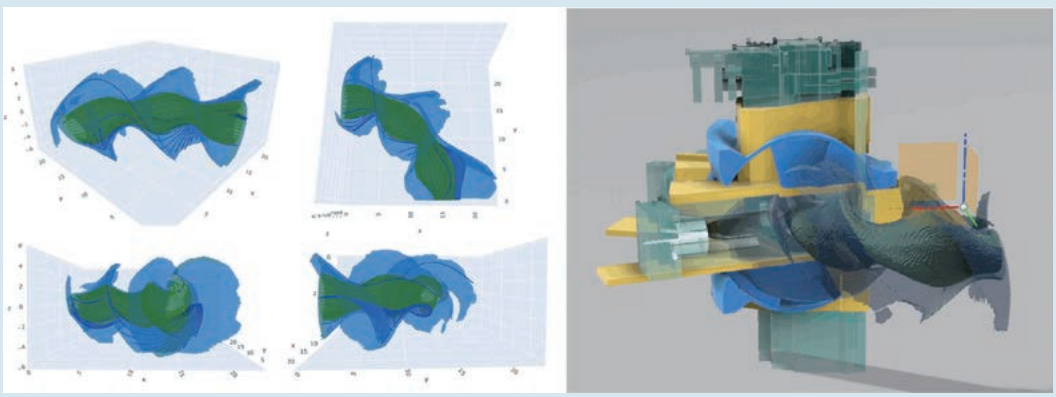

Fig. 1 On the left is a visualization result of a quarter of the plasma shape. The surface represents the edge surface layers and part magnetic field lines inside it, which are in blue, and the LCFS and part magnetic field lines inside it are in green. On the right is rendering result of the plasma shape and the fusion reactor.

(Kunqi Hu, Kyoto University)

Virtual-reality visualization of collision points of energetic tritons and plasma facing wall

The collision points of energetic tritons with a plasma facing wall of LHD are displayed with the divertor plates and vacuum vessel in a virtual-reality (VR) space, to research the distribution of the collision points [2]. The trajectory of the energetic tritons is calculated by the LOBIT code from the triton generation distribution given by the FIT3D-DD code. The trajectory calculation is performed without any collision effects under conditions in which the magnetic field is in a vacuum, the effect of the plasma is not included, and the electric field is negligibly small. Then the intersection points of the tritons and the plasma facing wall are detected. Each intersection point is stored in Cartesian coordinates. A point is visualized as a sphere by the Point-Sprite method in VR space with the rendered CAD data of divertor plates and the vacuum vessel. The points and CAD data are rendered by different visualization software, OpenGL-CAVE and Unity, respectively. The image data generated by the different software are captured and superimposed by a Fusion SDK. It is possible to investigate the distribution of the collision points on the divertor and vacuum vessel with realistic descriptions, shown in Fig. 2. This visualization helps the experiment researchers to determine the position of the material probe which catches the energetic tritons in real LHD experiments.

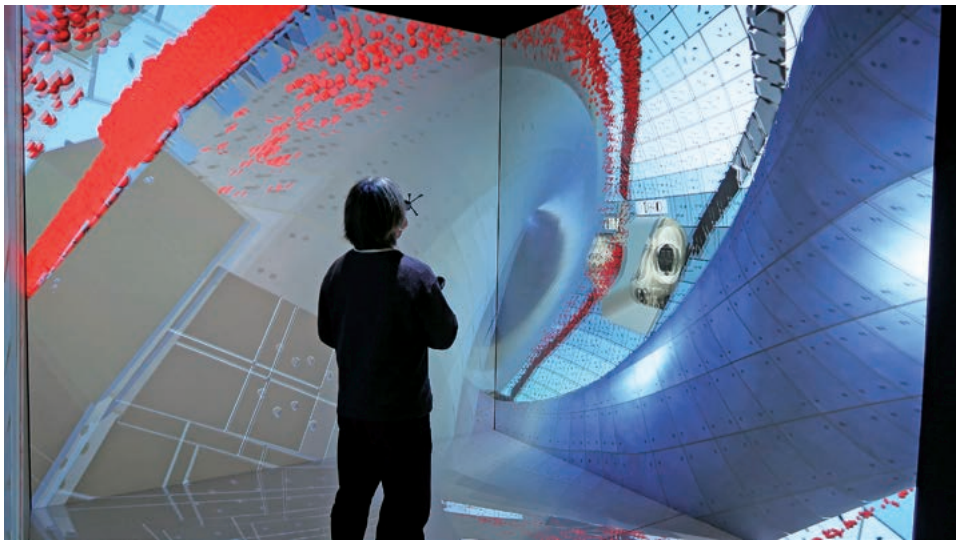

Fig. 2 The collision points of the energetic tritons and the plasma facing wall in LHD are visualized in the vacuum vessel in the VR space.

Development of the edge-based finite element method for investigation of high-temperature superconducting tape.

The permanent magnet method was proposed for measuring critical current density in HTS tape contactlessly and non-destructively. When a permanent magnet approaches and leaves the HTS tape, a shielding current is induced in the tape and the repulsive and attractive forces act on the permanent magnet, respectively. When the HTS tape is exposed to sufficiently large magnetic field, the shielding current becomes equal to the critical current and the repulsive and attractive forces are proportional to the critical current. Our developed numerical code, based on the edge-based finite element method, can evaluate the shielding current in the HTS tape and the force working on the permanent magnet, by solving the Maxwell equation with superconductivity characteristics. Figure 3 shows the dependence of the maximum force acting on the magnet on the number of the HTS tapes. When the magnetic flux density B_0 of the permanent magnet is 0.3T, the maximum force, F_M/F_{single}, is proportional to the number L of tapes for $L < 25$. On the other hand, when $B_0 = 1$T, F_M/F_{single} is proportional to L for $L < 40$. From this result, it is found that the permanent magnet method can measure the critical current density in multiple HTS tapes, and that the method has an upper limit of the number L of HTS tapes, in which the current density can be evaluated.

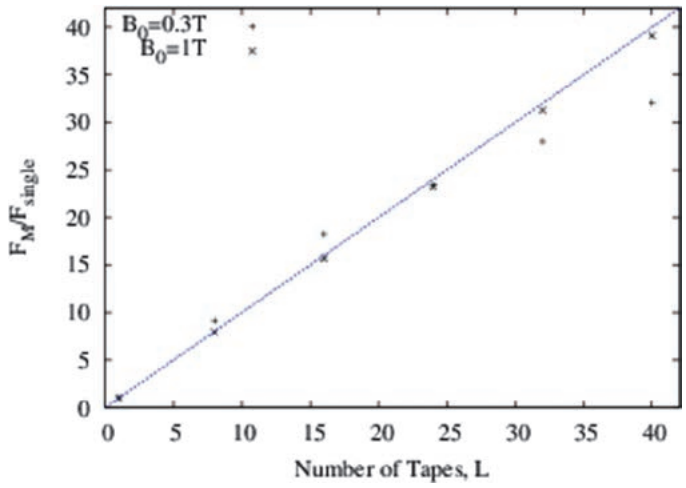

Fig. 3 Dependence of the maximum force, F_M, on the number of HTS tapes. The maximum force is divided by the value of the force, F_{single}, in a single HTS tape ($L = 1$). B_0 is a magnetic flux density of the permanent magnet.

[1] Kunqi Hu *et al.*, J. Visualization **24**, 1141 (2021).
[2] Hiroaki Ohtani *et al.*, J. Visualization **25**, 281 (2022).
[3] Takazumi Yamaguchi *et al.*, Plasma Fusion Res. **17**, 2405035 (2022).

(H. Ohtani)